COO-4946-3

STUDIES OF METAL - SEMICONDUCTOR INTERFACES IN CATALYSIS AND ENERGY CONVERSION

Annual Report

June 15, 1980 - June 14, 1981

Y. W. Chung

Northwestern University

Evanston, Illinois 60201

February 1981

Prepared For

The Department of Energy

Contract No.: DE-AC02-78ER04946

EAB

DISCLAIMER

NOTICE

ABSTRACT

Our experimental capability in the past year was enhanced considerably with the addition of a flame-ionization-detector gas chromatograph for the catalysis work, a high pressure mercury lamp for photochemical studies and a high resolution electron energy loss spectrometer for surface vibrational studies.

We showed that CO hydrogenation reactions can be performed reproducibly on a small area well characterized Ni (111) single crystal using an isolation cell technique. The activation energy for methane production (24.7 kcal/mole) and other hydrocarbon product distribution are in excellent agreement with the literature.

We demonstrated that Ni dispersed onto TiO_2(100) acquires a negative charge and that the Ni/TiO_2(100) exhibits a methanation activity at least 4 times that of Ni(111) with about the same activation energy. The Ni/TiO_2 also produces more higher hydrocarbons than Ni(111).

We examined the photochemical activity of Pt/$SrTiO_3$ in both aqueous solutions and in gas phase water. The activity in aqueous solutions under different conditions of pH and Pt coverage can be explained by band bending effects. A low hydrogen yield was observed in the presence of water vapor, and we attribute this to a slow photo-regeneration of active surface Ti^{3+}.

In collaboration with Professor Kesmodel of Indiana University, we performed preliminary high resolution electron energy loss studies on TiO_2(100) and observed strong surface phonon bands extending to 3000 cm^{-1}. This implies that better energy resolution is required to study adsorbate vibrations on these surfaces.

CONTENTS

1. INTRODUCTION

The format of this report is as follows. In section 2, we describe the improvements and additions of instrumentations used in our current research studies. In section 3, we present results of high pressure methanation studies on a well-characterized Ni(111) single crystal surface. In section 4, the methanation activity and product distribution of Ni/TiO_2 as a model catalyst-support system will be described. The photochemical activity of the $Pt/SrTiO_3$ system will be discussed in section 5. Finally, preliminary high resolution electron energy loss studies will be outlined in section 6. Sections 7 and 8 list respectively the publications and talks based on the present grant.

2. INSTRUMENTATIONS

Two major pieces of equipment were added this year. First, we installed a gas chromatograph (GC) equipped with a flame-ionization detector for our catalysis work. The output from the GC is further amplified ten times. The overall sensitivity of the whole GC setup to hydrocarbons depends, among other factors, on the volume of the reaction cell and the sample loop. In our case, a typical sensitivity for methane is $\sim 3 \times 10^{13}$ molecules. This allows us to study the catalytic methanation reaction down to 170°C.

A high-pressure mercury lamp is now in full operation and is the light source for all our photochemical studies on the $Pt/SrTiO_3$ system. The UV output intensity is adequate: at an input power of 240 watts, the photon intensity between 3.2 eV (bandgap energy of $SrTiO_3$) and 3.9 eV (cutoff of pyrex) is $\sim$ 160 milliwatts.

We are currently completing the installation of a high resolution electron energy loss spectrometer designed to have a resolution of $\sim$ 10 meV for vibrational studies (see section 6). The spectrometer will be interfaced to an Apple minicomputer for data acquisition and handling purposes.

3. METHANATION STUDIES ON Ni(111)

In the last grant period, we constructed an isolation cell attachment to an existing multi-technique ultrahigh vacuum (UHV) system. Using such a setup, we performed preliminary methanation experiments on a clean ordered Ni(111) single crystal (as determined by Auger electron spectroscopy and low energy electron diffraction). The success of these preliminary experiments demonstrated not only the feasibility of combining surface analytical techniques and high pressure catalytic studies using an isolation cell attachment, but also the wealth of information obtainable from such a synergistic approach.

Since then, we modified the isolation cell attachment slightly to enable a faster and more reliable specimen transfer between the UHV chamber and the cell. Also, we installed a flame-ionization-detector gas chromatograph that has excellent sensitivity for hydrocarbons e.g. the minimum detectable limit for methane is $\sim 3 \times 10^{13}$ molecules. This allows us to perform methanation reactions down to $\sim 170^{\circ}C$.

A typical run is shown in Figure 1, where we plot the number of methane molecules produced within the isolation cell versus time at an initial p_{H_2} = 60 Torr, p_{CO} = 20 Torr and a nickel crystal temperature of $200^{\circ}C$. The Ni(111) crystal area is 0.6 cm^2. At the end of the run, the cell was evacuated and the specimen introduced into the UHV chamber for Auger analysis. This transfer normally took less than five minutes. Figure 2a shows the presence of carbon and oxygen on the Ni surface after methanation. This is not surprising because the Ni surface was exposed to a high pressure of CO during methanation. Flashing the crystal to $300^{\circ}C$ removed the adsorbed CO, but a residual carbon peak remained (Fig. 2b). From the carbon Auger peak shape, the carbon is

Fig. 1 Methane production as a function of time on Ni(111)

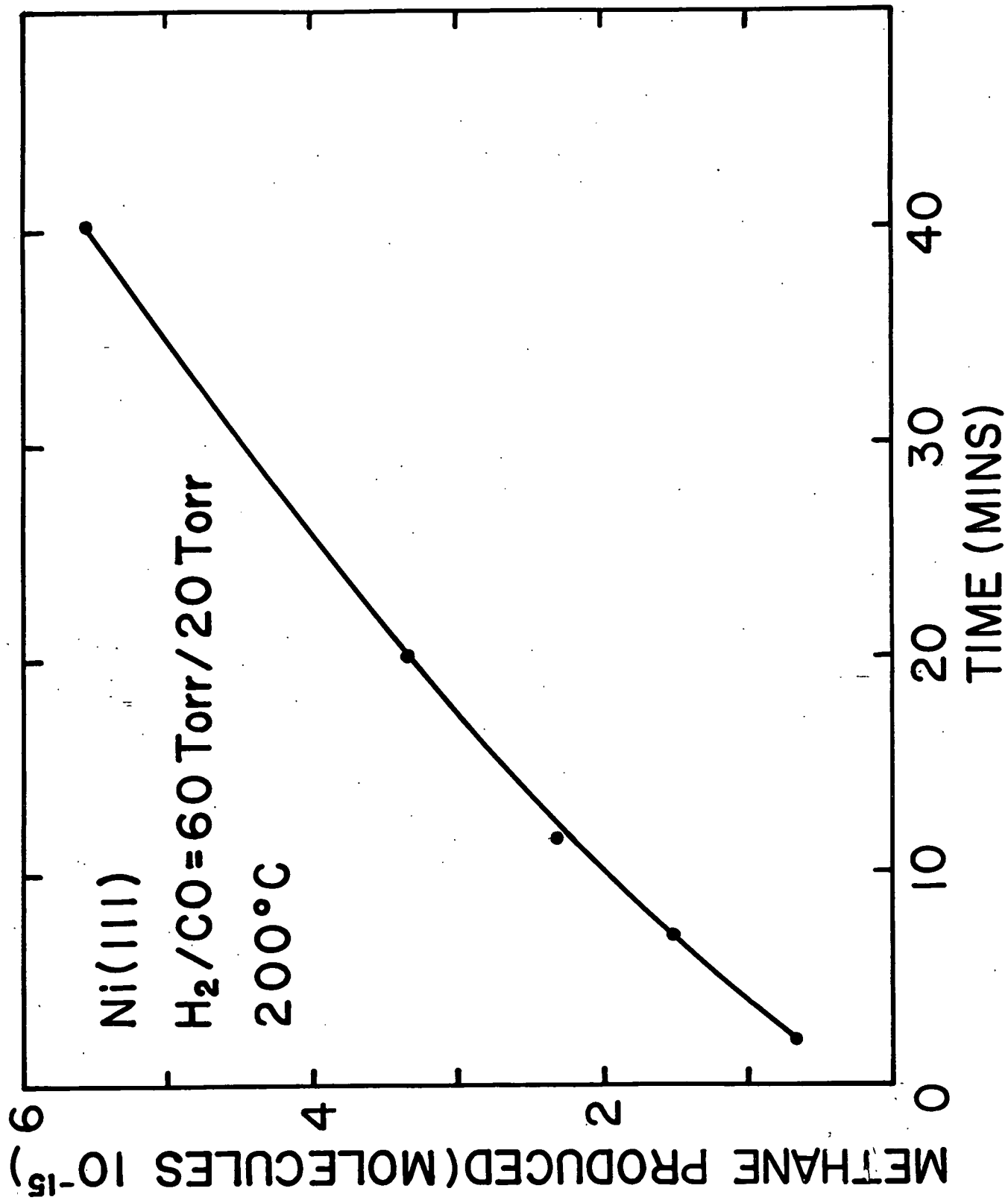

Fig. 2 Auger electron spectrum after methanation, following by flashing at 300°C.

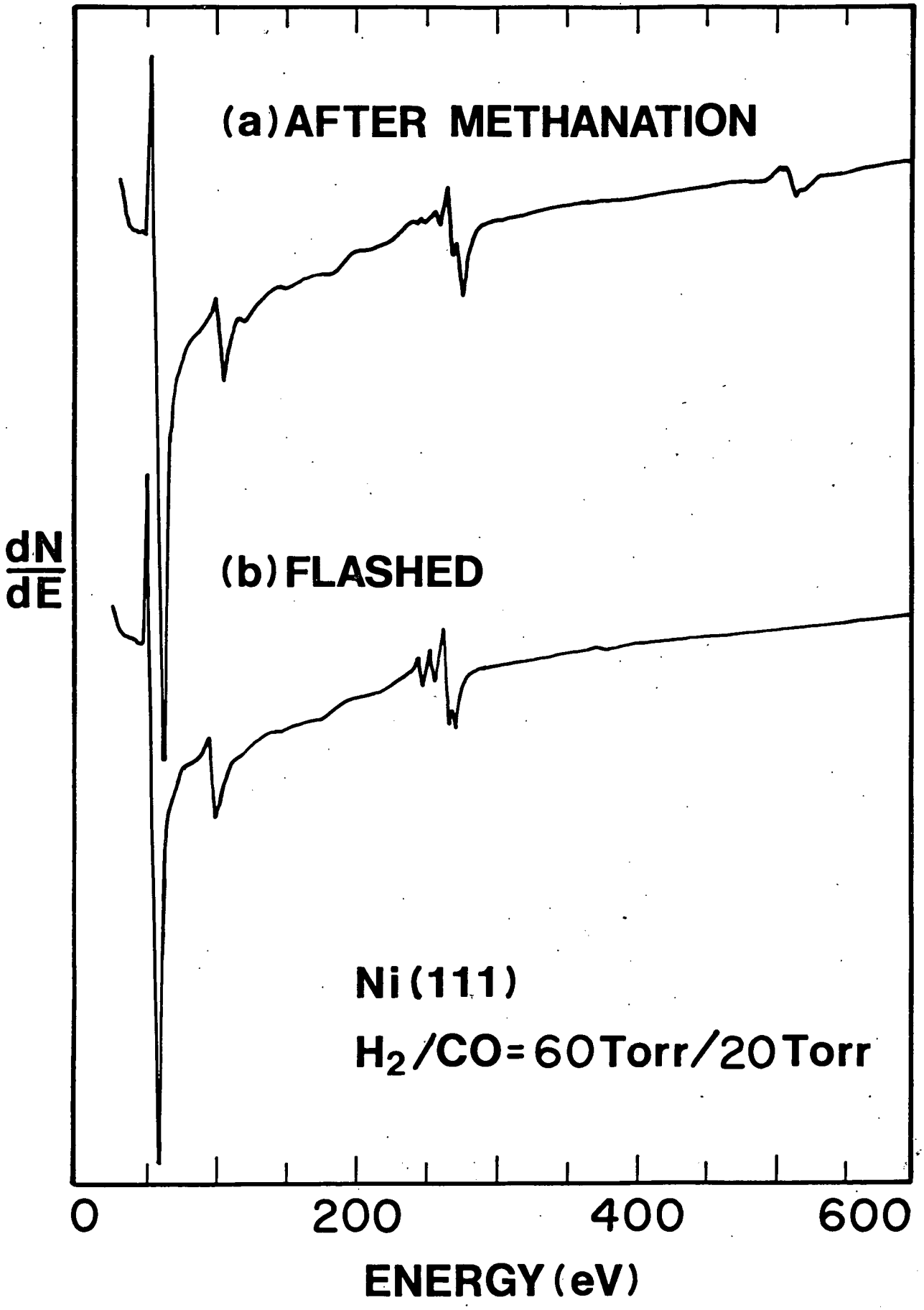

probably in the form of surface carbide, in agreement with the work of Krebs and Bonzel[1,2].

By performing the same reaction over a temperature range and obtaining the initial rate of methane production in each case, we obtained the Arrhenius plot of the methane turnover number (= number of methane molecules produced per Ni surface atom per second) versus temperature (Figure 3). All the data points fall almost perfectly on the same straight line. From the slope of the straight line, we obtained a value of 24.7 ± 0.6 kcal/mole for the activation energy. This is in good agreement with the result obtained by other workers on Ni/Al_2O_3[3] and single crystal nickel[4]. In addition, our methane turnover numbers over the temperature range 170-220°C agree to within 10% with those of the NBS group on single crystal nickel (100) and (111) under similar reaction conditions[4]. Such agreements are unheard of in the conventional catalysis literature. This again points to the advantage of applying surface science techniques to catalysis studies.

Figure 4 shows the corresponding hydrocarbon product distribution from Ni(111). The selectivity towards C_2 and C_3 products increases with decreasing temperatures. This is not unexpected because the free energy of formation of C_2 and C_3 products approaches that of methane as the temperature is decreased. Our observed product distribution is again in good agreement with that reported in current literature[3,5].

The above data of Ni(111) will serve as a reference for subsequent comparison with Ni/TiO_2, as well as studies of the isotope effect and sulphur poisoning.

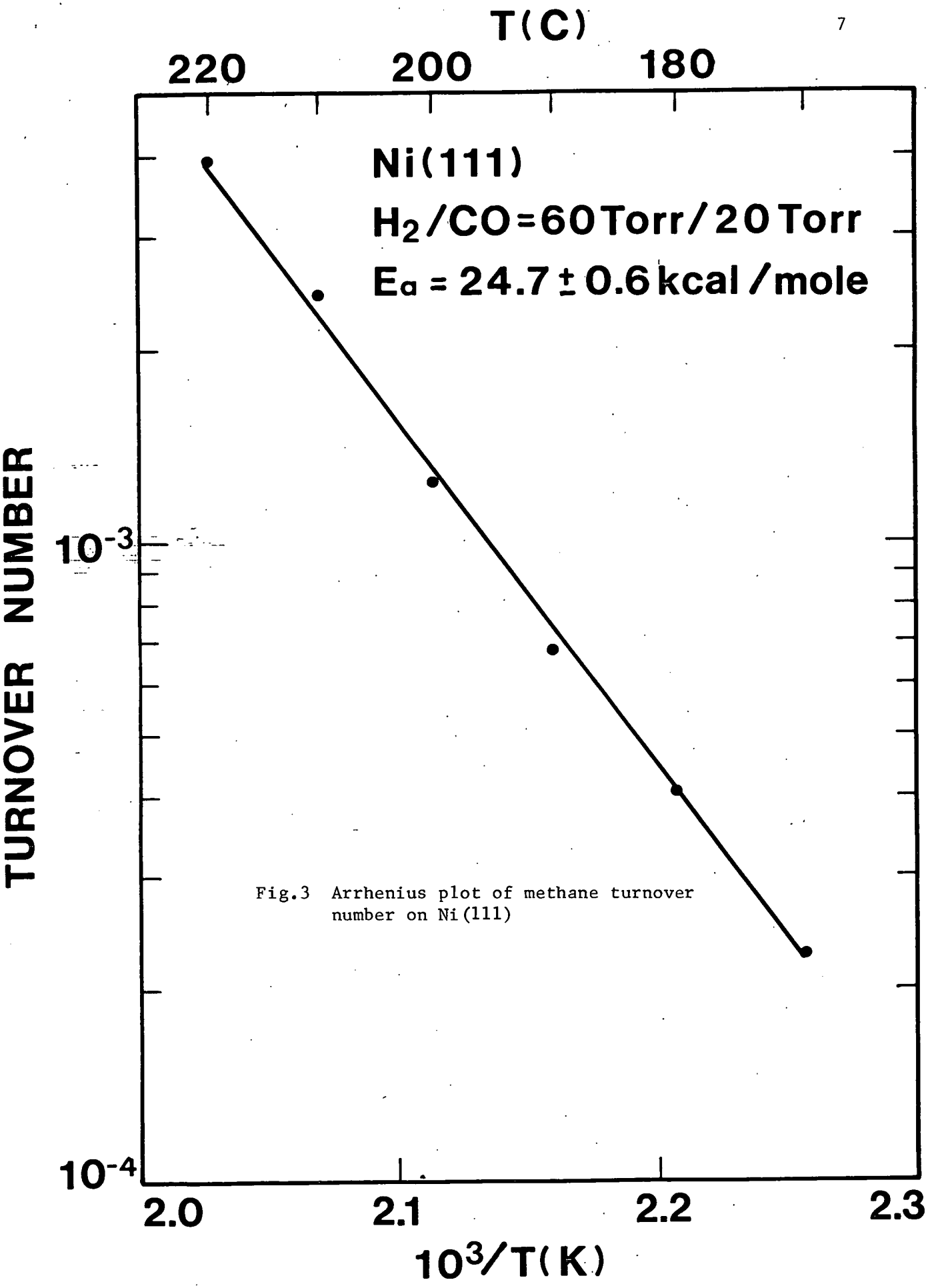

Fig.3 Arrhenius plot of methane turnover number on Ni(111)

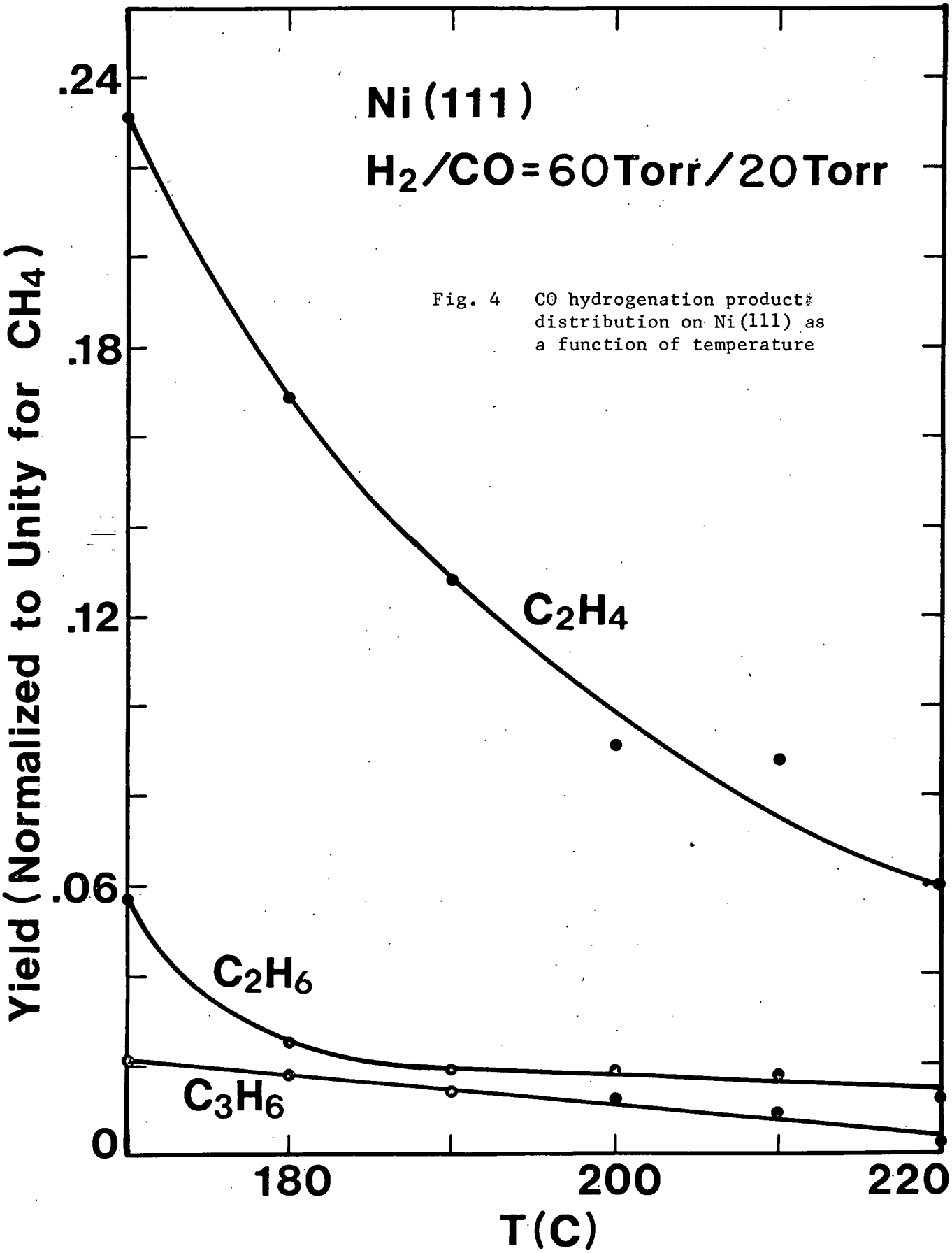

Fig. 4 CO hydrogenation product distribution on Ni(111) as a function of temperature

4. The Ni/TiO_2 System

Our previous studies showed that when nickel atoms are dispersed on the $TiO_2(110)$ surface, there is an electron transfer from TiO_2 to the surface nickel atoms, ~ 0.1 electron/nickel atom[6]. This change in the chemical state of the nickel atoms is expected to affect the chemisorption characteristics and catalytic activity of the Ni/TiO_2 system. Indeed, recent work by Tauster et al.[7] demonstrated the suppression of CO and H_2 chemisorption on transitional metals (Pt, Pd and Ir) supported on reduced TiO_2 surfaces. Vannice and Garten[8] showed that Ni/TiO_2 has a higher methanation activity and gives more higher hydrocarbons compared with unsupported Ni, Ni supported on graphite or Ni/Al_2O_3. These intriguing findings prompted us to examine the Ni/TiO_2 system in more detail.

Our ability to work with single crystal surfaces allows accurate determination of the surface composition and electronic properties and measurements of the geometric surface area, which is a necessary quantity to calculate turnover frequencies. The major problem is that Ni dissolves in TiO_2 quickly.[6] Fig.5 shows the Ni $2p_{3/2}$ level from a 2.1 monolayer of Ni on $TiO_2(110)$ and the same Ni $2p_{3/2}$ level after annealing at 300°C for 300 seconds. The dissolution of nickel is obvious. The dissolution problem is still present for Ni deposited on $TiO_2(100)$ but not as serious, probably because the (100) surface is closer-packed than the (110) surface. Thus, methanation reactions must be performed at less than 300°C to minimize the loss of nickel.

(a) Charge transfer between Ni and TiO_2(100)

By measuring the Ni $2p_{3/2}$ core level and the Ni $L_3M_{2,3}M_{2,3}$ Auger kinetic energy shift as the nickel coverage on $TiO_2(100)$ goes from 0.5

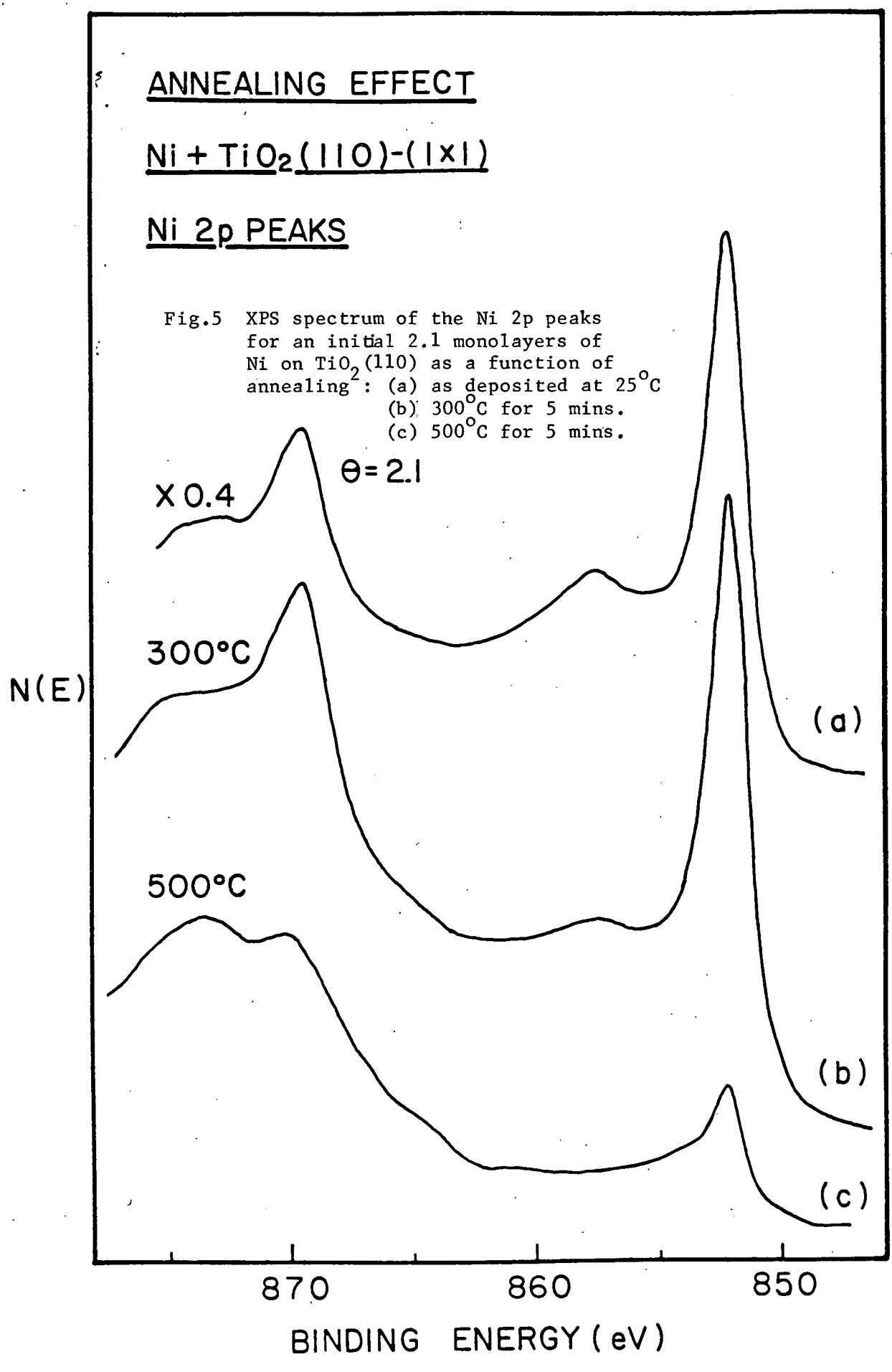
ANNEALING EFFECT
Ni + TiO2(110)-(1x1)
Ni 2p PEAKS
Fig.5 XPS spectrum of the Ni 2p peaks for an initial 2.1 monolayers of Ni on TiO2(110) as a function of annealing: (a) as deposited at 25°C (b) 300°C for 5 mins. (c) 500°C for 5 mins.
X 0.4
θ = 2.1
300°C
500°C
N(E)
(a)
(b)
(c)
870
860
850
BINDING ENERGY (eV)

monolayer to 15. monolayers, we estimate[6] using the same procedure we developed previously an electron transfer from TiO_2(100) to Ni ~ 0.1 electron/Ni surface atom, similar to that for Ni/TiO_2(110). Therefore, the nickel atoms are negatively charged.

(b) Dissolution of Ni in TiO_2

To estimate the amount of nickel lost in the course of the methanation reaction, we deposited approximately 1.5 - 2.0 monolayers of nickel onto TiO_2(100) and monitored the nickel 61 eV Auger intensity as a function of time over the temperature range 170°C - 220°C. Results show that even in the worse case (220°C), there is still more than one monolayer of nickel on the surface after 10 minutes of heating.

(c) CO Hydrogenation on Ni/TiO_2

We performed CO hydrogenation reactions on Ni/TiO_2 under the following conditions using the isolation cell attachment to an existing ESCA/Auger/UPS/LEED chamber:

Sample: 1.5 - 2.0 monolayers of nickel vapor-deposited on a clean TiO_2(100)-(1 x 3) surface at a substrate temperature of 160°C

Reactants: P_{CO} = 20 Torr

P_{H_2} = 60 Torr

Using a gas chromatograph equipped with a flame-ionization detector, we measured the number of hydrocarbon molecules produced as a function of time. To minimize the loss of nickel, we limited the reaction temperature to the range of 170°C - 220°C. As a result, we can only detect up to C_3 hydrocarbons.

The result of this study is exciting. Fig. 6 shows the Arrhenius plot of the methane turnover number versus temperature. Again, all the data points fall almost perfectly on the same straight line. From the slope of the straight line, we estimated an activation energy of 25.3 ± 0.2 kcal/mole , which is almost the same as that for nickel (111) and agrees closely with the result of Vannice and Garten[9]. More importantly, the methane turnover number for Ni/TiO_2 is always higher than that for Ni(111) under identical reaction conditions (by a factor of 4-5). Note that the turnover number shown in fig. 6 is calculated on the assumption that the number of surface nickel atoms is the same as that on Ni(111), viz. 1.86×10^{15} nickel atoms/cm^2, and therefore represents a lower-limit estimate of the actual turnover number for the Ni/TiO_2 system.

Fig. 7 shows the corresponding hydrocarbon product distribution from $Ni/TiO_2(100)$. The selectivity towards C_2 and C_3 products increases with decreasing temperatures, as expected. Further, Ni/TiO_2 produces more C_2 and C_3 hydrocarbons than Ni(111) under identical conditions.

The implications of these findings are far-reaching. We have obtained irrevocable evidence that nickel atoms dispersed on TiO_2 are more active in the CO hydrogenation reaction, giving more methane and higher hydrocarbons than Ni(111) under the same reaction conditions. If the observation that the nickel atoms in contact with TiO_2 are negatively charged accounts for this activity enhancement, then it would be fruitful to manipulate the initial TiO_2 surface properties, thus altering the charge on the Ni atoms and correlate this with its catalytic activity. We are currently continuing our research studies with this objective.

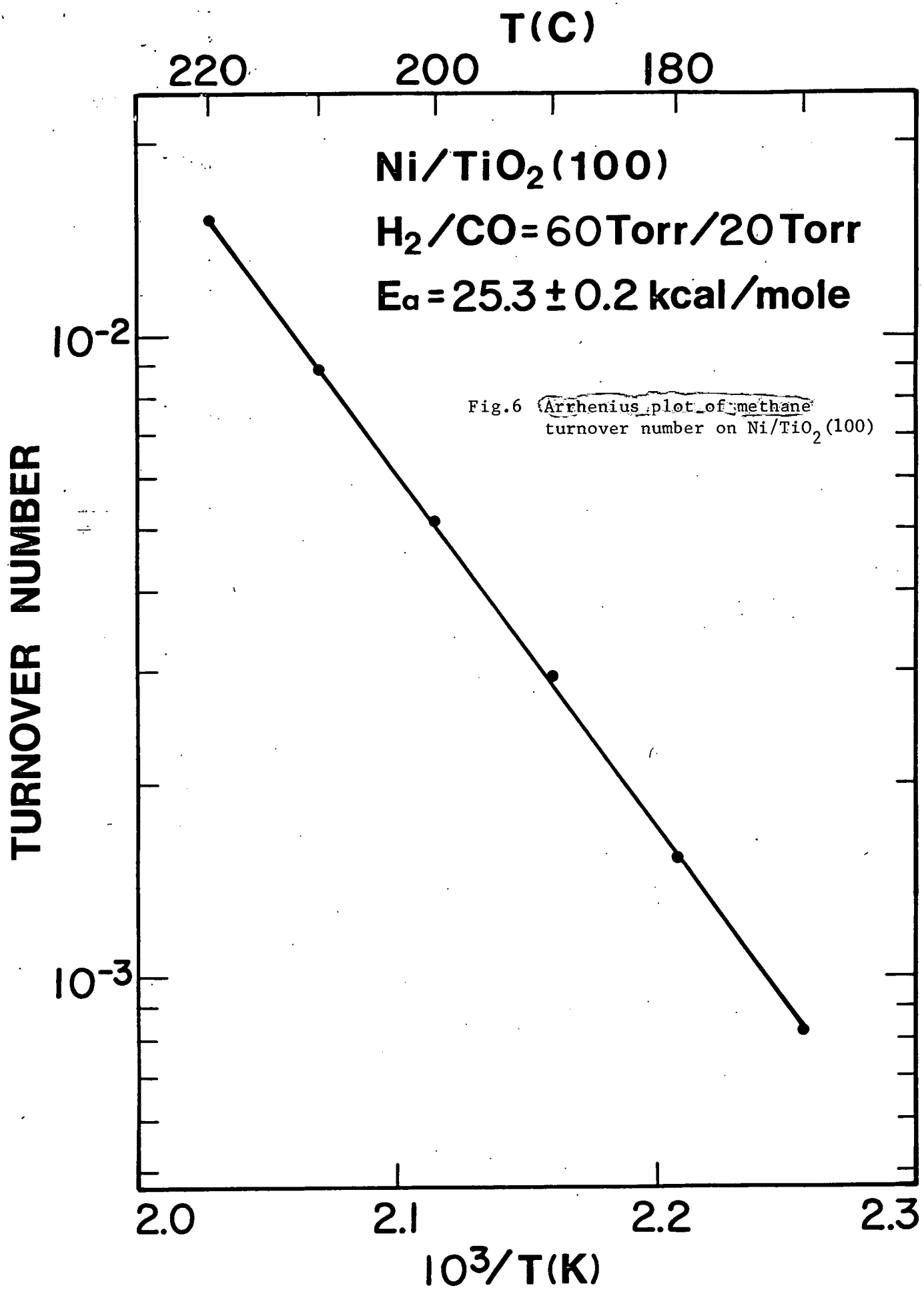

Fig.6 Arrhenius plot of methane turnover number on $Ni/TiO_2(100)$

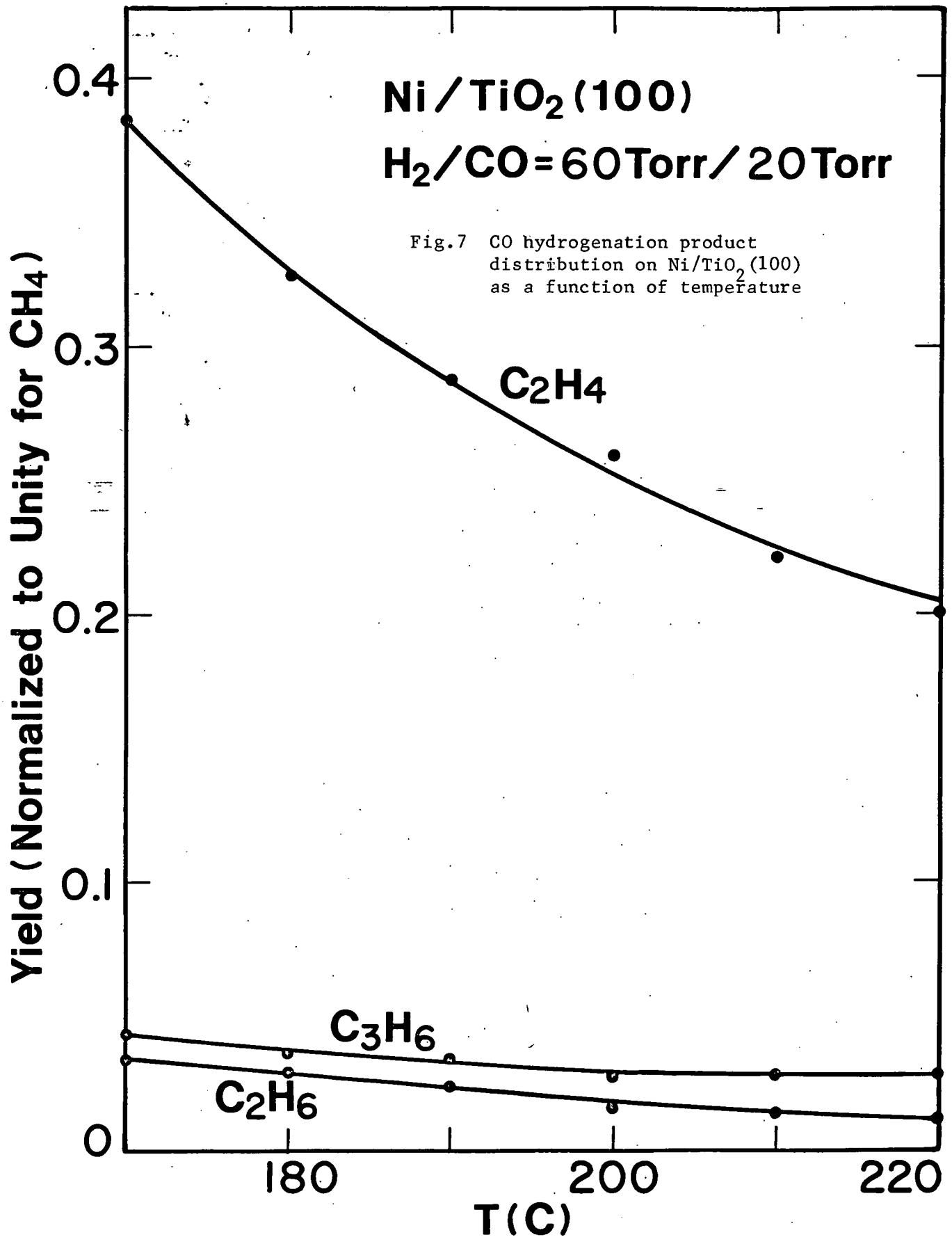

Fig.7 CO hydrogenation product distribution on $Ni/TiO_2(100)$ as a function of temperature

5. The $Pt/SrTiO_3$ system

Our previous photoemission studies[10,11] showed that when Pt is deposited onto a clean $SrTiO_3(100)$ surface, there is an electron transfer from $SrTiO_3$ to Pt and a Schottky barrier of height 0.4 eV is formed. In the current period, we investigated how this Schottky barrier between Pt and $SrTiO_3$ affects the photoassisted decomposition of water in the aqueous solution.

The experimental setup is sketched in fig. 8. An isolation cell was attached to a Physical Electronics PHI 548 ESCA/Auger chamber. The specimen was prepared inside this main chamber, characterized with LEED and AES and then transferred by an introduction rod from the main chamber to the isolation cell where all photochemical reactions were performed. The isolation cell consists of a six-way cross with a sapphire or pyrex window mounted on one end. Its inner wall was coated with gold to avoid contamination and background reactions. The gas sample was analyzed by a thermal conductivity gas chromagraph (GC). The overall sensitivity of the GC setup for hydrogen is two monolayers. The result of the study is summarized in Table 1.

Table 1

Hydrogen production rate from $SrTiO_3$ and $Pt/SrTiO_3$ under different conditions. The incident photon flux (between 3.2 and 3.9 eV) is 160 mW.

		H_2 production rate*
(i)	$SrTiO_3$ in water	75 ± 10 monolayers/hour
(ii)	$Pt/SrTiO_3$ in water	60 ± 10 monolayers/hour
(iii)	$SrTiO_3$ in 5N NaOH	90 ± 10 monolayers/hour
(iv)	$Pt/SrTiO_3$ in 5N NaOH	275 ± 10 monolayers/hour

* 1 monolayer is defined as 1×10^{15} molecules

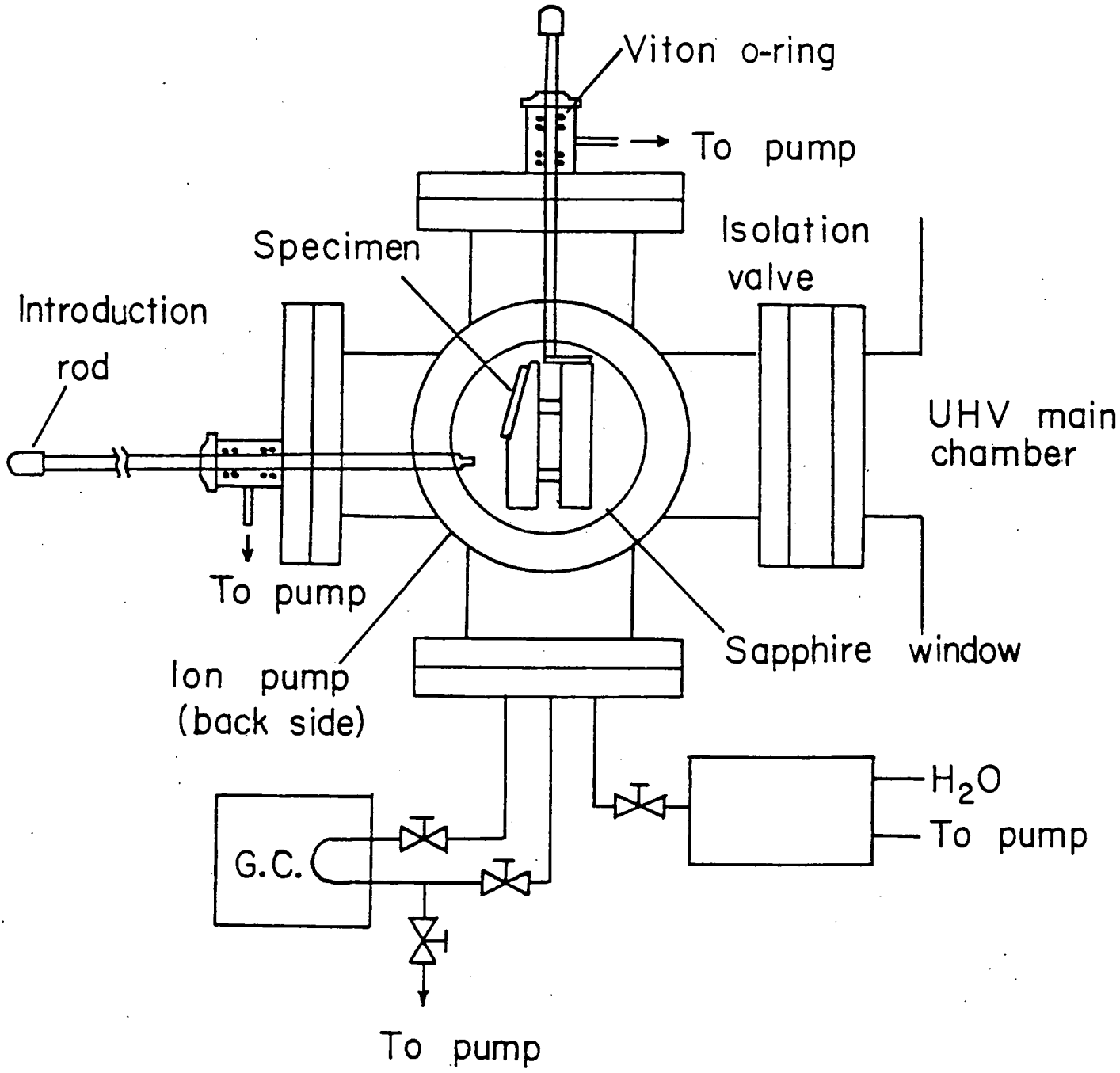

Fig. 8 The isolation cell setup

The variation of hydrogen yield in the above four cases can all be attributed to band bending effects:

Case (i) The band bending at the $SrTiO_3$/water interface is 0.5 eV. When illuminated with intense bandgap radiation, this band bending is reduced to zero so that the separation of the photogenerated electron-hole pairs is not favorable, hence the low hydrogen yield.

Case (ii) There is a barrier of 0.4 eV at the Pt/$SrTiO_3$. When illuminated with intense bandgap radiation, the band bending at the Pt/$SrTiO_3$ and the $SrTiO_3/H_2O$ interface will both be reduced. When the Pt/$SrTiO_3$ barrier is reduced to zero, the band bending at the $SrTiO_3/H_2O$ interface is 0.1 eV, which is small for efficient separation of photogenerated charge carriers.

Case (iii) Similar to case (i).

Case (iv) The situation here is different. In this case, while the Pt/$SrTiO_3$ barrier is still the same (0.4 eV), the $SrTiO_3$/5N NaOH band bending is larger (1.0 eV). Bandgap illumination can remove the Pt/$SrTiO_3$ barrier while still maintaining a substantial band bending at the $SrTiO_3$/5N NaOH interface to effect charge separation and hence results in an increased yield. Since electron injection into the electrolyte to produce hydrogen is only possible when the quasi-Fermi level of Pt coincides with the H_2/H^+ redox potential level (E_{redox}), the steady state band bending at the $SrTiO_3$/NaOH interface is $E_{cb} - E_{redox}$ ($\simeq$ 0.3 eV), E_{cb} being the energy location of the $SrTiO_3$ conduction band minimum[12]. This is sufficiently large to enable efficient electron-hole separation.

Therefore, in photo-reactions using Pt-free $SrTiO_3$, no appreciable steady state band bending at the $SrTiO_3$/electrolyte interface could be achieved. For Pt/$SrTiO_3$, the initial (before illumination) band bending at the SrTi03/electrolyte interface has to exceed that at the Pt/$SrTiO_3$ interface by 0.3 eV to eventually achieve sufficient band bending at the $SrTiO_3$/electrolyte interface on illumination.

We attempted the photodecomposition of water vapor on the 1-cm^2 $SrTiO_3$ (100) surface covered with 0.5 monolayer of Pt. We observed a slow but sustained hydrogen production of 2×10^{15} molecules/hr. at an incident photon flux ($h\nu$ = 3.5 eV) of 1×10^{15}/sec. This is consistent with the results of previous studies on TiO_2 powders[13] and the Pt/TiO_2 systems[14], in which no or low hydrogen production was observed when water vapor was used. One possible reason for this low hydrogen yield is the occurence of the fast back-reaction in the gas phase. To examine this possibility, we repeated the above experiment by introducing about 500 monolayers of hydrogen and oxygen into the isolation cell and monitoring the hydrogen signal by the G.C. The amount of hydrogen in the isolation cell did not change with UV illumination. Thus back-reaction is not among the factors contributing to this low hydrogen yield.

We believe that the major reason is the slow regeneration of the active surface Ti^{3+} species. Studies by the Berkeley group show that surface Ti^{3+} species can be generated by the bandgap illumination but the time constant of this process is large, ~ 1000 seconds[15-17]. That is, the Ti^{3+} regeneration rate is on the order of $3 \times 10^{15}/cm^2$-hr, in good agreement with the observed hydrogen production rate. Therefore, to enhance the hydrogen production rate, one must devise additional channels for the generation of active surface Ti^{3+} species.

6. PRELIMINARY HIGH RESOLUTION ELS STUDIES

High resolution electron energy-loss spectroscopy involves the detection of quantum vibrational energy losses (or gains) due to the interaction of an incident, highly monochromatic electron beam of energy 1 - 10 eV with surface phonons or molecular vibrations of an adsorbed species. Electron spectrometers with the necessary energy resolution of 5 - 15 meV, first employed in this area by Ibach and co-workers[18], have recently been constructed by a number of research groups.

This technique is especially powerful in determining the effect of a titanium oxide support on the surface chemical properties of nickel atoms dispersed on the oxide surface. To initiate this effort, we first constructed the high resolution spectrometer based on a design supplied by Dr. Brett A. Sexton[19]. The spectrometer is now completed, a picture of which is shown (Figure 9). The spectrometer is based on the electrostatic 127° cylindrical sector, one sector serving as the electron monochromator and the other as electron analyzer. The sectors and lenses were precision-machined from OFHC copper and coated with colloidal graphite to reduce stray electron scattering. The spectrometer optics is rigidly held in place by machinable ceramic rods and spacers and is shielded with μ-metal foils to reduce the residual magnetic field to less than 30 mG. The spectrometer and the specimen holder are both mounted on an aluminum base attached to an 8" OD-conflat flange. Each sector of the spectrometer is designed to achieve an energy revolution of 0.7%.

Parallel to this construction effort is a preliminary study of surface vibrations on $TiO_2(100)$[20]. This work was performed in collaboration with

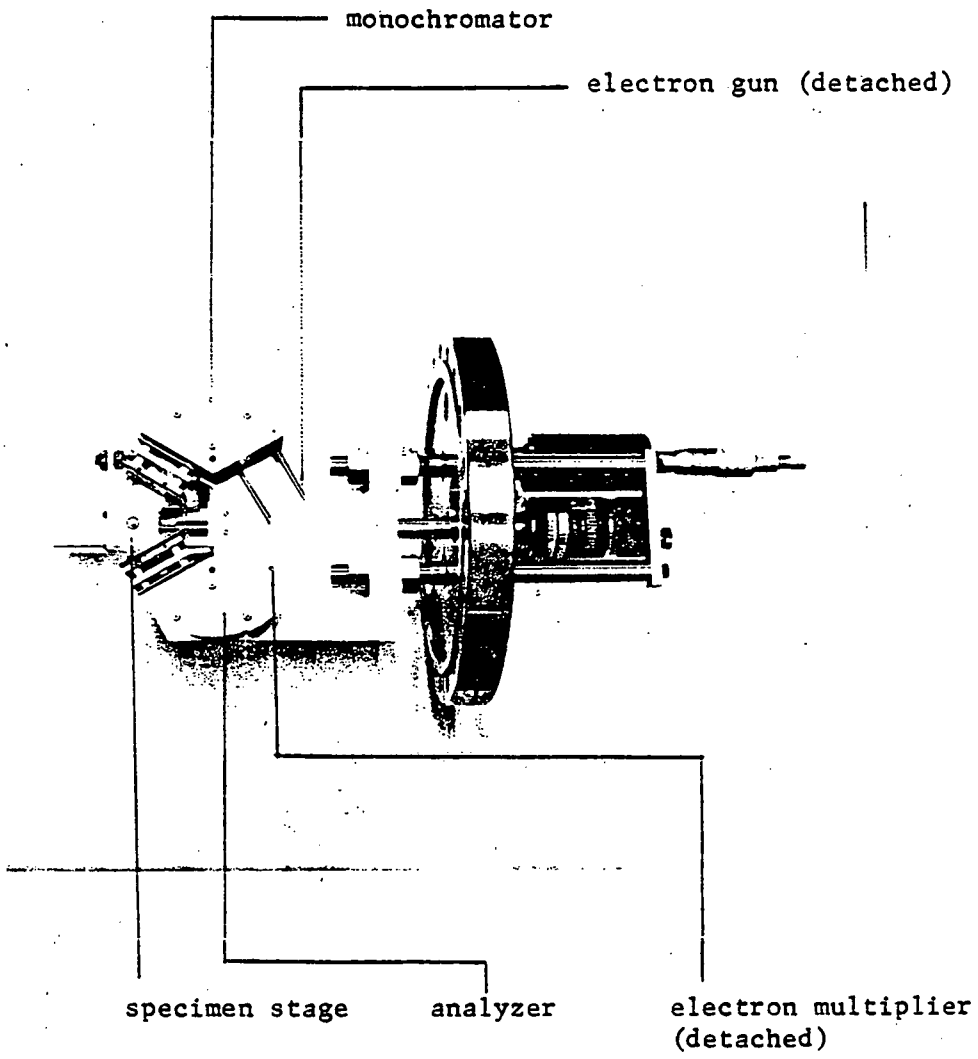

Fig.9 The high resolution ELS spectrometer

Professor L. L. Kesmodel of Indiana University, using his spectrometer. A typical electron energy loss spectrum of TiO_2(100) near room temperature is shown in Figure 10. The spectrum was obtained on the specular reflection at an incident beam energy of 14 eV and incident angle of 50° from the surface normal. Two principal loss features are observed at 436 cm^{-1} and 766 cm^{-1}. There are also weaker and broader loss features observed in the 1000-3000 cm^{-1} range as well as energy gain peaks at 436 and 766 cm^{-1}. If one interprets the loss peaks at 436 cm^{-1} and 766 cm^{-1} as surface optical phonons with frequencies ν_1 and ν_2 respectively (this interpretation is justified by model calculations), then all the other spectral features can be attributed to multiple and combination phonon losses.[20] Moreover, the ratio of the intensity of the one-phonon energy gain peaks to the one-phonon loss peaks agree with the Boltzmann factor $\exp(-h\nu_i/k_BT)$ within experimental error.

It is important to note that the presence of relatively strong multiple phonon bands extending to $\sim$ 3000 cm^{-1} will make the detection of many adsorbate vibrations on these surfaces difficult. A better energy resolution with our spectrometer should minimize this problem.

Fig. 10 EELS spectrum of TiO_2 (100) at an electron incident energy of 14 eV. The signal is detected in the specular direction

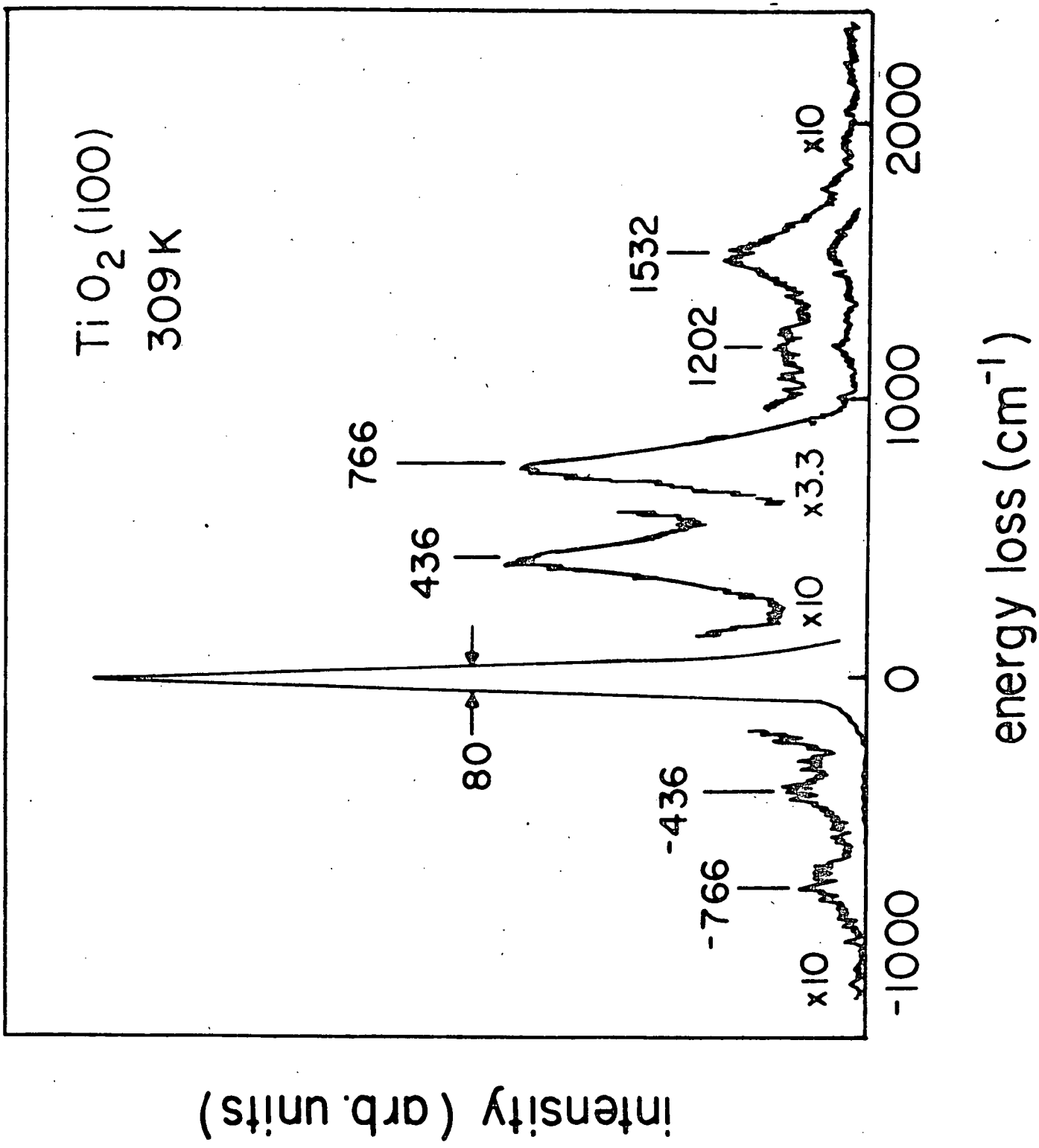

7. Publications based on present grant

1. M. K. Bahl, S. C. Tsai and Y. W. Chung, "Auger and photoemission investigations of the Pt-$SrTiO_3$(100) interface: relaxation and chemical shift effects", Physical Review B21, 1344 (1980).

2. C. C. Kao, S. C. Tsai, M. K. Bahl, Y. W. Chung and W. J. Lo, "Electronic properties, structure and temperature-dependent composition of nickel deposited onto rutile titanium dioxide (110) surfaces", Surface Science 95, 1 (1980).

3. L. L. Kesmodel, J. A. Gates and Y. W. Chung, "Observation of surface optical phonons on TiO_2(100)", Physical Review B 23, 489 (1981).

8. Talks based on present grant

1. "Surface science studies of metal-support interactions", Exxon Corporate Research Laboratories, New Jersey, March 1980.

2. "Surface defect properties of rutile titanium dioxide", Solid state seminar, Indiana University, April 1980.

3. "Surface science studies of metal-support interactions", Chicago Catalysis Club Symposium, Chicago, May 1980.

4. "Surface electronic properties of nickel atoms dispersed on rutile TiO_2 surfaces as a model catalyst-support system", 40th Physical Electronics Conference, Cornell University, June 1980.

5. "Application of XPS to semiconductors", Society for Applied Spectroscopy Multidisciplinary Symposium, Chicago, October 1980.

9. Miscellaneous

Time devoted by the Principal Investigator

100% time for 1½ summer months (1980)

20% time for the academic year

REFERENCES

1. H. J. Krebs and H. P. Bonzel, Surf. Sci. 88, 269 (1979).

2. H. P. Bonzel and H. J. Krebs, Surf. Sci. 91, 499 (1980).

3. M. A. Vannice, J. Catalysis 44, 152 (1976).

4. D. W. Goodman et al., J. Catalysis 63, 226 (1980).

5. M. A. Vannice, J. Catalysis 37, 449 (1975).

6. C. C. Kao et al., Surf. Sci. 95, 1 (1980).

7. S. J. Tauster, S. C. Fung and R. L. Garten, J. Am. Chem. Soc. 100, 170 (1978).

8. M. A. Vannice and R. L. Garten, J. Catalysis 56, 236 (1979).

9. M. A. Vannice and R. L. Garten, J. Catalysis 66, 242 (1980).

10. Y. W. Chung and W. B. Weissbard, Phys. Rev. B20, 3456 (1979).

11. M. K. Bahl, S. C. Tsai and Y. W. Chung, Phys. Rev. B21, 1344 (1980).

12. J. M. Bolts and M. S. Wrighton, J. Phys. Chem. 80, 2641 (1976).

13. G. N. Schrauzer and T. D. Guth, J. Am. Chem. Soc. 99, 7189 (1977).

14. S. Sato and J. M. White, Chem. Phys. Letters 72, 83 (1980).

15. W. J. Lo, Y. W. Chung and G. A. Somorjai, Surf. Sci. 71, 199 (1978).

16. Y. W. Chung, Ph.D. Thesis, LBL-6625, Lawrence Berkeley Laboratory (1977).

17. S. Ferrer and G. A. Somorjai, Surf. Sci. 94, 41 (1980).

18. See, for example, H. Froitzheim, in Electron Spectroscopy for Surface Analysis, ed. H. Ibach (Springer, Berlin, 1977).

19. B. A. Sexton, J. Vac. Sci. Tech. 16, 1033 (1979).

20. L. L. Kesmodel, J. A. Gates and Y. W. Chung, Phys. Rev. B23, 489 (1981).